# We are IntechOpen,
# the world's leading publisher of
# Open Access books
# Built by scientists, for scientists

## 6,900
Open access books available

## 186,000
International authors and editors

## 200M
Downloads

## 154
Countries delivered to

Our authors are among the

## TOP 1%
most cited scientists

## 12.2%
Contributors from top 500 universities

**CLARIVATE ANALYTICS**
**BOOK CITATION INDEX**
**INDEXED**

**WEB OF SCIENCE**™

Selection of our books indexed in the Book Citation Index
in Web of Science™ Core Collection (BKCI)

## Interested in publishing with us?
## Contact book.department@intechopen.com

**2**

# Application of Electrochemical Techniques and Mathematical Simulation in Corrosion and Degradation of Materials

Jorge González-Sánchez, Gabriel Canto,
Luis Dzib-Pérez and Esteban García-Ochoa
*Centre for Corrosion Research,*
*Autonomous University of Campeche,*
*Mexico*

## 1. Introduction

The tropical climate prevailing at Yucatan Peninsula in Mexico is characterized by permanently high temperatures and relative humidity with considerable precipitation, at least during part of the year. A high corrosion rate of metals is usually reported for this climate and for marine conditions the corrosion degradation of infrastructure is an issue of paramount importance.

This chapter presents studies about the degradation of some engineering materials, such as austenitic stainless steels (localised corrosion in chloride containing electrolytes) and atmospheric corrosion of copper and nickel-iron alloys from both approaches experimental electrochemical tests and theoretical calculations respectively. The evaluation of the corrosion process of stainless steels in chloride containing solutions and atmospheric corrosion of copper in a marine tropical-humid climate are presented and discussed making emphasis on the electrochemical techniques used. On the other hand, a computational simulation indicated weakening of metal bonds in Fe-Ni (111) surfaces due to interaction with CO after adsorption of this compound. The union weakening observed can be associated with alloy embrittlement by the decohesion mechanism.

It is worth mentioning that one important contribution of the "Disciplinary research group: Corrosion Science and Engineering" of the Centre for Corrosion Research of the Autonomous University of Campeche, MEXICO has been the use for the very first time of the recursive plots methodology for the analysis of current and potential time series from electrochemical noise measurements for studies of localised corrosion. With such approach it was possible to assess changes in the dynamics of the degradation process and to separate the contribution of different phenomena.

Novel electrochemical techniques and advanced methods for data analysis are the base for the understanding of thermodynamic and kinetics aspects involved on the corrosion degradation of engineering materials such as copper, carbon steel and stainless steels. Electrochemical noise (EN), galvanostatic cathodic reduction (CR), scanning reference

electrode technique (SRET), double loop electrochemical potentiokinetic reactivation method (DLEPR) and electrochemical impedance spectroscopy (EIS) are some of the electrochemical methods used to study the corrosion degradation process of stainless steels and other engineering metals.

The SRET has been used for the quantitative assessment of localized dissolution of AISI 304 stainless steel in natural seawater and in 3.5% NaCl solution at room temperature (25 °C) (González-Sánchez, 2002; Dzib-Pérez, 2009). Changes in the dynamics of intergranular corrosion of AISI 304 stainless steel as a function of the degree of sensitisation (DOS) was evaluated by EN using recurrence plots for the analysis of current time series (García-Ochoa et al., 2009). Also the microstructure dependant short fatigue crack propagation on AISI 316L SS was distinguished from localised corrosion taking place during corrosion fatigue tests using EN (Acuña et al., 2008).

The information presented here was divided in two main sections: Atmospheric corrosion and Localised corrosion, followed by a final section of general conclusions.

## 2. Atmospheric degradation of engineering alloys

### 2.1 Atmospheric corrosion of Cu in tropical climates

Degradation of engineering alloys due to atmospheric corrosion is the most extended type of metal damage in the world. During many years, several papers have been published in this subject; however, most of the research has been made in non-tropical countries and under outdoor conditions. Tropical climate is usual on equatorial and tropical regions and is characterized by high average temperature and relative humidity with considerable precipitation during the major part of the year. Due to these conditions a high corrosion rate of metals is usually reported for this type of climate. In coastal regions like the Gulf of Mexico (Yucatan Peninsula), there is a natural source of airborne salinity which plays an important role in determining corrosion aggressivity of these regions (Mendoza & Corvo, 2000; Cook et al., 2000). The presence of anthropogenic contaminants, particularly sulphur compounds produced at the oil and manufacture industries and transportation have also an important effect on the atmospheric corrosivity of tropical-humid regions. The atmospheric corrosion rate of metals depends mainly on the time of wetness (TOW) and concentration of pollutants; however, if the differences in the corrosion process between outdoor and indoor conditions are taken into account, the influence of direct precipitation such as rain is very important for outdoor and negligible for indoor conditions. The acceleration effect of pollutants could change depending on wetness conditions of the surface, so the influence of the rain time and quantity should be very important in determining changes in corrosion rate (Corvo et al., 2008).

Dew or humidity condensation is considered a central cause for the corrosion of metals. Its formation depends on the relative humidity (RH) and on the changes of temperature. Because dew does not wash the metallic surface, the concentration of pollutants becomes relatively high in the thin layer of electrolyte and could be much more aggressive than rain. Rain gives rise to the formation of a thick layer of water and also adds corrosive agents such as $H^+$ and $SO_4^{2-}$, however it can wash away the contaminants as well. It does depend on the intensity and duration of the rainfall.

Corvo et al., made some recommendations in order to improve the methodology for estimation of TOW-ISO which include among others the establishment of limit of air temperature ranges dividing it in two categories: from 0 °C to 25 °C and higher than 25 °C. Also the inclusion of time and amount of rain as an additional variable, taking into account the washing and cleaning effect of rain, limiting the use of TOW-ISO to outdoor and not highly contaminated environments (Corvo et al., 2008).

Together with the assessment of atmosphere corrosivity, the actual corrosion rate of metals must be evaluated in order to have the complete body of information about the phenomenon. The rate of atmospheric corrosion of metals is evaluated mainly by two procedures: the gravimetric method (mass loss measurements) and using electrochemical techniques like cathodic reduction measurements, electrochemical impedance spectroscopy, electrochemical noise and potentiodynamic polarization. Electrochemical techniques are applied to assess the corrosion rate of metals exposed to the atmosphere and to other aggressive environments because they provide instantaneous corrosion rate values and in most of the cases can be considered as non-intrusive methods. For example linear sweep voltammetry and cathodic reduction (Chronopotentiometry) are two electrochemical techniques that have been successfully used for the quantitative analysis of copper oxides formed during the atmospheric corrosion of this metal (Nakayama, 2001, 2007).

On the other hand, electrochemical noise (EN) was used as a novel approach to study atmospheric corrosion as it is able assess the protective properties of the corrosion products formed on metal surfaces. This technique involves the recording of current fluctuations taking place between two similar electrodes separated by a wetted cloth; one electrode is the surface under evaluation whilst the other is a clean non-corroded sample of the same metal. The current or potential fluctuations measured are associated with the electrochemical behaviour of the corroded metal. It can be considered as a nonintrusive technique as the metal sample is not perturbed by any electrical signal. The EN methodology has been applied successfully for the study of atmospheric corrosion in artificial and natural atmospheres giving information on the severity and morphology of the attack as a function of time (García-Ochoa et al., 2008, Torres et al., 2006).

Electrochemical Noise measurements were applied to study the protection level offered by corrosion products formed on samples of Cu exposed in different outdoor atmospheres during a relatively short periods. Also chronopotentiometric measurements (Cathodic reduction) were conducted to determine the presence of different copper compounds forming the patinas. The results from EN measurements in terms of the noise resistance (Rn) were consistent with the corrosion rate obtained from mass loss measurements and cathodic reduction as shown in figure 1, (García-Ochoa et al., 2008).

Cathodic reduction test (galvanostatic cathodic polarisation) applied on samples in an oxygen free KCl solution gave corrosion rate values very similar to those calculated from electrochemical noise and mass lose measurements.

Samples of Cu were exposed short time periods at 7 different outdoor sites. The micro-climates of these sites had remarkable effect on the atmospheric corrosion of Cu and on the kind of corrosion products formed on the surface. Electrochemical noise analysis allowed assessing the protective characteristics of the corrosion products which is related to the corrosion process and the quantity of dissolved metal.
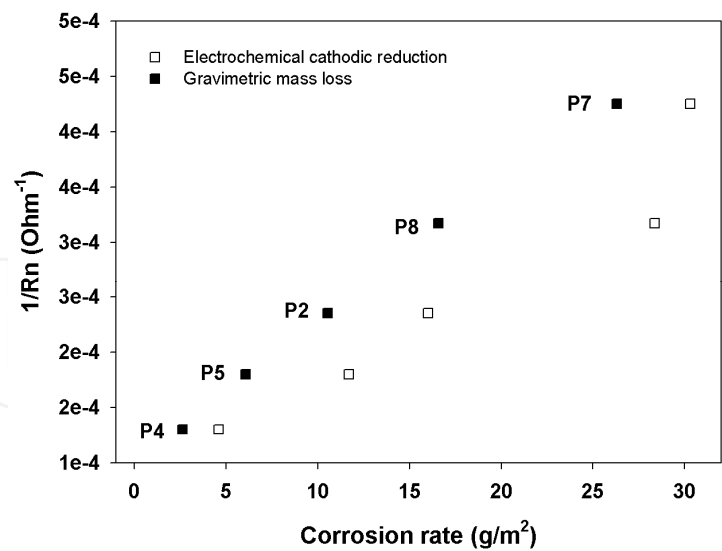
Fig. 1. The Rn values plotted against corrosion rate (gm-2) obtained from mass loss and cathodic reduction tests.

The inflection points observed in the potential vs time curves gave information of the kind of compound reduced during the polarisation and the time at which the inflections appear is the time used to calculate the quantity of corroded metal as shown in Figure 2. A plateau at around -1,146 mV is clearly defined. This plateau has been associated with the presence and reduction of $Cu_2S$, which is a crystalline compound that has a more negative reduction potential than the copper oxides (Itoh et al., 2002, Watanabe et al., 2001). The cathodic reduction results indicated a major presence of sulphur compounds in sample 7.
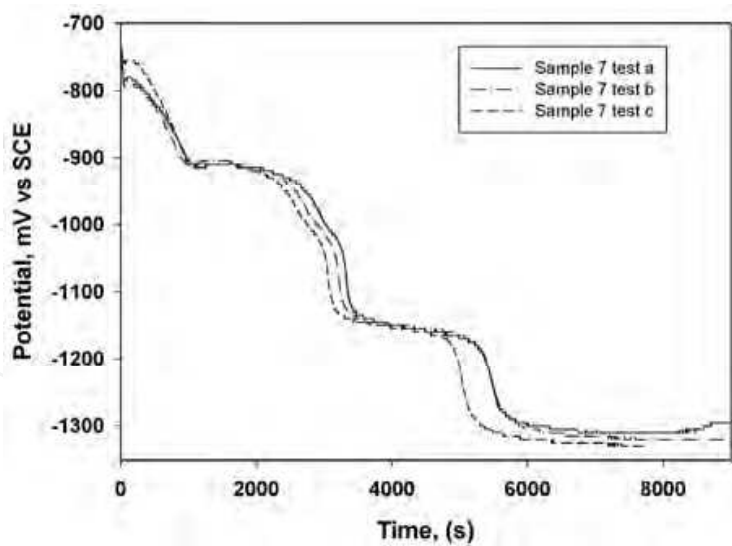


Fig. 2. Potential–time curves from galvanostatic polarisation of Cu samples in 0.1 M KCl.

The electrochemical noise technique was able to evaluate the protection level of corrosion products formed on copper samples during a relatively short exposure period to different outdoor atmospheres in terms of Rn. This parameter showed a proportional relationship with the aggressiveness of the atmosphere. The application of electrochemical noise using

two electrodes offers the possibility of determining the sites where corrosion is more intense, the higher the amplitude of the signal, the higher the corrosion rate. This methodology permits evaluation using the natural surface electrolyte formed during atmospheric corrosion. The three different methods used to evaluate the atmospheric corrosion of copper: gravimetric analysis, electrochemical noise (Rn), and chronopotentiometry indicate the same pattern as a function of the exposure site. Using cathodic reduction it was possible to determine the presence of copper sulphide in the copper corrosion products, indicating the significant influence of $H_2S$ in the atmospheric corrosion of copper.

Atmospheric degradation of engineering materials takes place also in dry conditions in which electrochemical reactions are not involved (electrochemical corrosion). This other form of degradation involves metallic surface-gas interactions. In order to get an insight of this phenomenon, theoretical and simulation studies of molecular level are carried out for different groups around the world. The case of the effect of CO adsorbed on the degradation of a Ni-Fe alloy is presented in the next sub-section.

## 2.2 A computational study of CO adsorption on a Ni-Fe surface

The materials used for industrial process are generally Fe- and Ni-based alloys that offer high corrosion and creep resistance. However, when the material is exposed to gases containing carbon, e.g. CO, it can pick up carbon (Grabke, 1998). The resistance to thermal cycling is reduced and there is a danger of cracks developing in the material. In consequence, the understanding of the interaction of carbon monoxide with nickel-iron alloys can be useful in order to reduce this undesirable behavior.

As an example, a combination of flow reactor studies and electron microscopy techniques has been used to investigate the way the composition of iron-nickel alloy particles influence the growth characteristics of carbon deposits formed during the decomposition of ethane at temperatures over the range 815–865 °C. Major differences in the selectivity patterns of alloys were evident with the amount of solid carbon catalytically produced being significantly higher on a Fe–Ni (5:5) powder than on a Fe–Ni (8:2) sample. Examination of the deposit revealed the existence of two types of structures, carbon nanofibers and a graphite shell-like material, both of which contained associated metal particles (Rodriguez et al., 1997). The information on literature about studies of the adsorption of CO on Fe/Ni alloys at quantum level is quite limited. This section presents a study of the CO chemisorption on a FeNi(111) surface based on calculations in the framework of the Density Functional Theory (DFT) (Hohenberg & Kohn, 1964).

The exchange-correlation potential ($V_{XC}$) considered within the generalized gradient approximation (GGA) proposed by Perdew et al., (Perdew et al., 1996) and the self-consistent total energy method, as implemented in the SIESTA Package code (Ordejon et al., 1996), has been used here. This methodology has been successfully applied for the study of several kinds of interactions (Sánchez-Portal et al., 2004). The electron–ion interactions are treated by means of norm conserving pseudopotentials in accordance with the Troullier-Martins procedure (Troullier & Martins, 1991). For the base set, a double zeta basis set plus polarization functions (DZP) was used. The atomic orbitals were slightly excited (0.01 Ry) in order to limit the range of the pseudo-atomic base orbitals (Sankey & Niklewski, 1989).

A uniform grid in real space with a mesh cutoff of 450 Ry was used for calculations. The Brillouin zone was sampled, and total energy converged correspondingly to the number of k points resulting in the Monkhorst-Pack matrix diagonal (7×7×1) (Monkhorst & Pack 1976).

To understand the interactions between the atoms, we used the concept of COOP (Crystal Orbital Overlap Population) curves. A COOP curve is a plot of the overlap population weighted DOS (density of states) vs. energy. The integration of the COOP curve up to the Fermi level ($E_f$) gives the total overlap population of the bond specified and it is a measure of the bond strength.

The interaction between the CO molecule and the FeNi(111) surface was studied using a two dimensional slab of finite thickness in order to have the best simulation of the semi-infinite nature of the metallic surface. A three-layer slab was employed as a compromise between computational economy and reasonable accuracy. The FeNi(111) surface was represented by a 108 atoms (50:50) distributed in three layers (FCC arrangement). It was found the final configuration of the CO/FeNi(111) system using the Spanish Initiative for Electronic Simulations with Thousands of Atoms (SIESTA) method (Soler et al. 2002). A geometry optimization was performed applying relaxation calculations. The top two layers of the substrate were allowed to relax together with the adsorbate while the bottom layer was kept fixed in the bulk position. Table 1 presents the C-surface distances and the relative minimum energy corresponding to the CO location for each adsorption site by SIESTA calculations.

| Adsorption Site | C-surface distance (Å) | Relative Energy (eV) |
| --- | --- | --- |
| 1 | 1.79 | 0.58 (L) |
| 2 | 1.83 | 0.41(L) |
| 3 | 1.40 | 0.19 (NL) |
| 4 | 1.20 | 0.00 (NL) |
| 5 | 1.43 | 0.278 (L) |
| 6 | 1.38 | 0.232 (L) |
| 7 | 1.38 | 0.069 (NL) |

L: local minimum energy

NL: no local minimum energy

Table 1. Carbon-surface distances calculations and, carbon-surface distance, relative energy and type of the minimum energy position by SIESTA calculations for the CO adsorption sites on the FeNi(111) surface.

The 1, 2, 5 and 6 sites present a local minimum energy showing the molecule optimum localization at these sites. On the other hand, the 3, 4 and 7 sites are not stable and correspond to transition states, since CO relaxes to other sites when initially put at these ones. Finally, the most stable location for CO on the FeNi(111) surface corresponds to an intermediate position between 1 and 4 sites, where the C atom is positioned in the middle of two Ni atoms and a neighbouring Fe atom. A schematic view of the CO location is shown in Figure 3 (bottom).
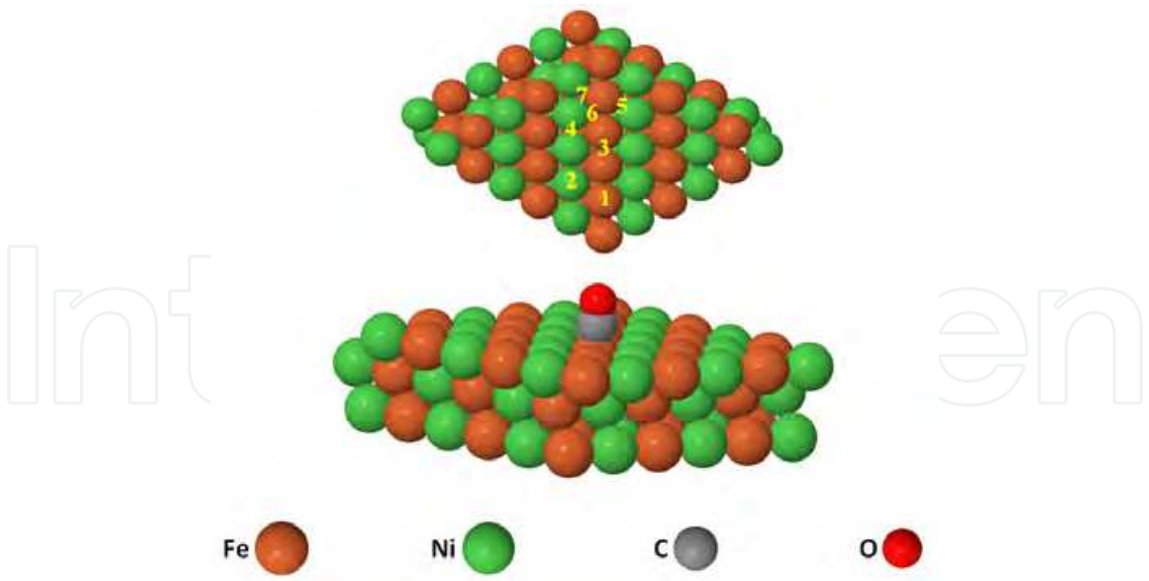
Fig. 3. Schematic (a) initial sites for CO adsorption and (b) final view of the CO location, on the FeNi(111) surface

For the final configuration a C-O distance of 1.20 Å and a C-surface distance of 1.35 Å were found which are in agreement with results reported for the adsorption of CO on both Fe and Ni single crystal surfaces, respectively (Jiang & Carter, 2004; Karmazyn et al., 2003; Gajdoš et al., 2004; Peters et al., 2001). For the electronic structure calculations, the density of states (DOS) and the crystal orbital overlap population (COOP) curves for the CO/FeNi(111) system were determined in order to analyze the adsorbate-surface interactions. Figure 4 (middle) shows the DOS plots for the CO/FeNi(111) system.
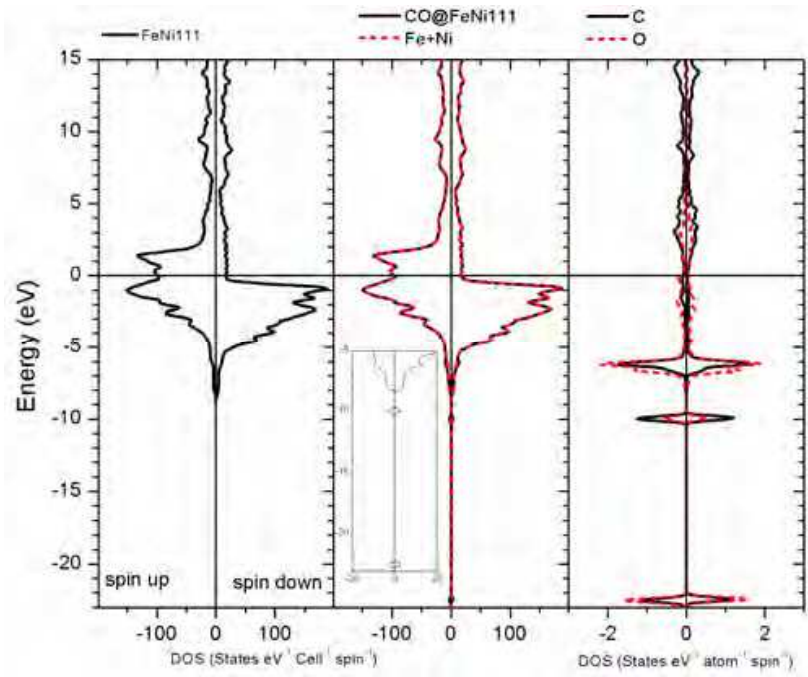


Fig. 4. Total DOS for the CO/FeNi(111) system (middle), total DOS for the clean FeNi(111) surface (left) and projected DOS for CO on the FeNi(111) surface (right).

The small contribution of the CO to total DOS is due to its low concentration. For a major view, Figure 4 (right) presents a plot of CO states projection after adsorption. To understand the interactions between the atoms, concept of COOP (crystal orbital overlap population) curves was used. The atomic orbital occupation and the OP values for the atoms that participate in the absorbate-substrate interactions were also calculated (see Table II).

| Atom | Orbital occupation | | | Charge | Bond | Distance (Å) | OP |
|------|------|------|------|--------|------|------|------|
|      | s | p | d |        |      |      |      |
| $Fe_{nn}$ | 0.765 | 0.622 | 6.537 | 0.076 [a] | $Fe_{nn}$-C | 2.09 | 0.185 [a] |
|      | 0.848 | 0.591 | 6.477 | 0.084 [b] | $Fe_{nn}$-NN | ------ | 0.803 [a] |
|      |       |       |       |           |             |        | 0.941 [b] |
| $Ni_{nn}$ | 0.788 | 0.856 | 8.503 | -0.147 [a] | $Ni_I$-C | 1.94 | 0.246 [a] |
|      | 0.871 | 0.735 | 8.494 | -0.100 [b] | $Ni_I$-NN | ------ | 0.845 [a] |
|      |       |       |       |           |           |        | 0.989 [b] |

[a] In the CO@Feni(111)

[b] In the FeNi(111)

nn: nearest neighbor to C

NN: up to 3rd nearest neighbor in the metallic surface

Table 2. Atomic orbital occupations and net charges for the CO neighboring Fe and Ni atoms, and the corresponding OP values and distances by SIESTA calculations.

The C (of the CO molecule) bonds with nearest neighbors Ni and Fe surface atoms reported Ni-C (1.94 Å) and Fe-C (2.09 Å) OP values of 0.246 and 0.185, respectively. Compare these new interactions with the metal-metal interaction (isolated FeNi matrix), the Ni-C and Fe-C interactions have OP values that correspond to 25 % and 20 % of the metallic bond OP, respectively. The COOP curves for the new interactions correspond to mainly bonding interactions as can be seen in Figure 5.
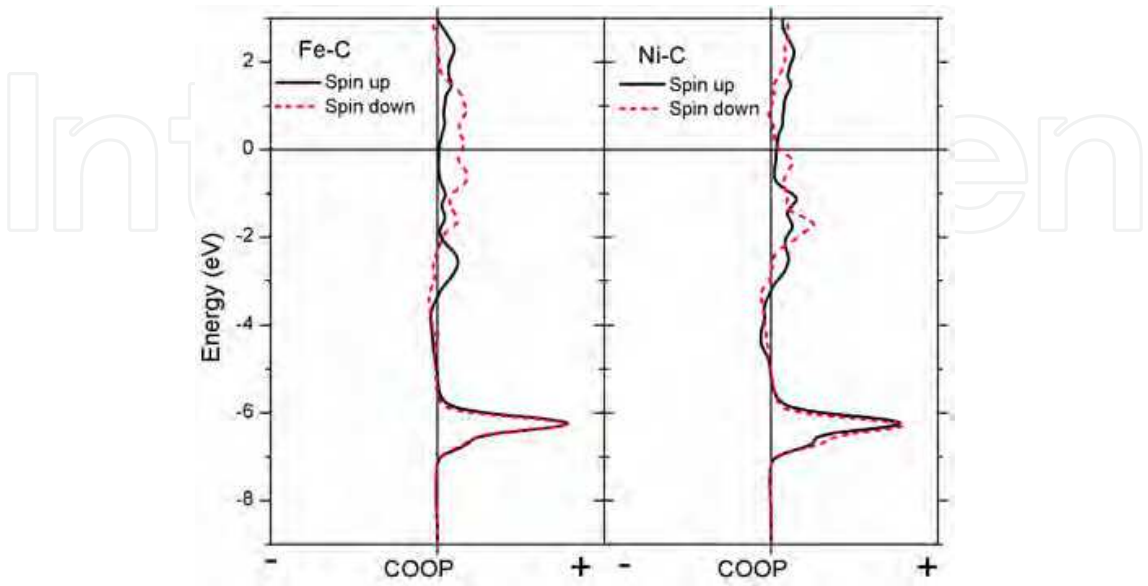


Fig. 5. COOP curves for Fe-C and Ni-C interactions.

The substrate-adsorbate interactions mainly involve the s and p orbitals of Ni whose populations decrease 9.53 % and increase 16.46 %, respectively compared with a clean surface. The Ni d orbital populations only decrease to about 0.11 %. On the other hand, the Fe orbital occupations are modified and the major changes are also noticed in the s and p atomic orbitals whose populations decrease 9.78 % and increase 5.24 % respectively, after CO adsorption. The Fe d populations only decrease to about 0.93 %. In general, there is observed an electron transfer from CO to the Fe and Ni nearest neighbors, then the surface-layer of the slab is negatively charged relative to the bulk due to CO interaction (see Table II). A large bonding OP between C and both Ni and Fe atoms appears, while the Ni–Ni, Fe-Fe and Ni-Fe OP decrease. After CO adsorption, the strength of the Ni-NN and Fe-NN bonds (NN: metallic atoms up to 3rd nearest neighbor) decreases to about 15 %. A detrimental effect on the metal bonds is observed after CO adsorption on the FeNi(111) surface and can be associated with the alloys embrittlement by decohesion mechanism.

## 3. Localised corrosion

### 3.1 Localised corrosion of stainless steels

Stainless steels are basically iron–chromium–nickel alloys, containing between 18 and 30 wt% chromium, 8–20 wt% nickel and 0.03–0.1 wt% carbon. According to metallurgical structure stainless steels are divided into three groups: austenitic "γ" face centred cubic (fcc), ferritic "α" body centred cubic (bcc), and martensitic (body centred tetragonal or cubic). There is another stainless alloy, duplex ("γ - α"), which possesses a two-phase microstructure with approximately equal amounts of austenite and ferrite (Marshall, 1984).

Austenitic stainless steel of the series 300 such as the UNS 30400 (S30400 SS) is used in a wide range of applications due to its acceptable corrosion resistance in non-chloride containing environments and good weldability. This kind of steel loses its corrosion resistance when is cooled slowly from the solution anneal temperature around 1273 K (1000 °C) or is reheated in the range from 823 K (550 °C) to 1123 K (850 °C). In this temperature range there is a tendency to precipitate chromium-rich carbides as the alloy enters the carbide plus austenite phase field (Marshall, 1984; Lacombe et al., 1993). Precipitation of carbides such as $M_{23}C_6$ and $M_7C_3$ occurs primarily at the austenite grain boundaries which are heterogeneous nucleation sites. The chemical composition in the vicinity of the grain boundaries can be altered by the precipitation of the chromium rich particles (Lacombe et al., 1993). This phenomenon is called sensitization and prompts the resulting chromium-depleted zones at the grain boundaries to be susceptible to intergranular corrosion (Terada et al., 2006). This is a well known form of localised corrosion on stainless steels in particular on sensitised austenitic grades and look like the examples presented in Figure 6.

There are several published works about the corrosion of stainless steels which deal with different metal-electrolyte systems using different electrochemical techniques (Burstein, 2004; Curiel, 2011; Isaacs, 1989; Newman, 2001; Sudesh, 2007; Turnbull, 2006). Localised attack in the form of crevice and pitting corrosion is the most insidious and common initiation stage for the development of cracks under static or cyclic mechanical loading (Zhou, 1999; Akid, 2006; González-Sánchez, 2002; Acuña, 2005).

The effect of sensitisation on the corrosion resistance of stainless steels is difficult to determine quantitatively using conventional polarisation electrochemical methods, owing to

the negligible weight loss involved. The microscopic dimension of the chromium depleted zone next to the grain boundaries is overshadowed by the unaffected bulk of the grains in many conventional corrosion tests.
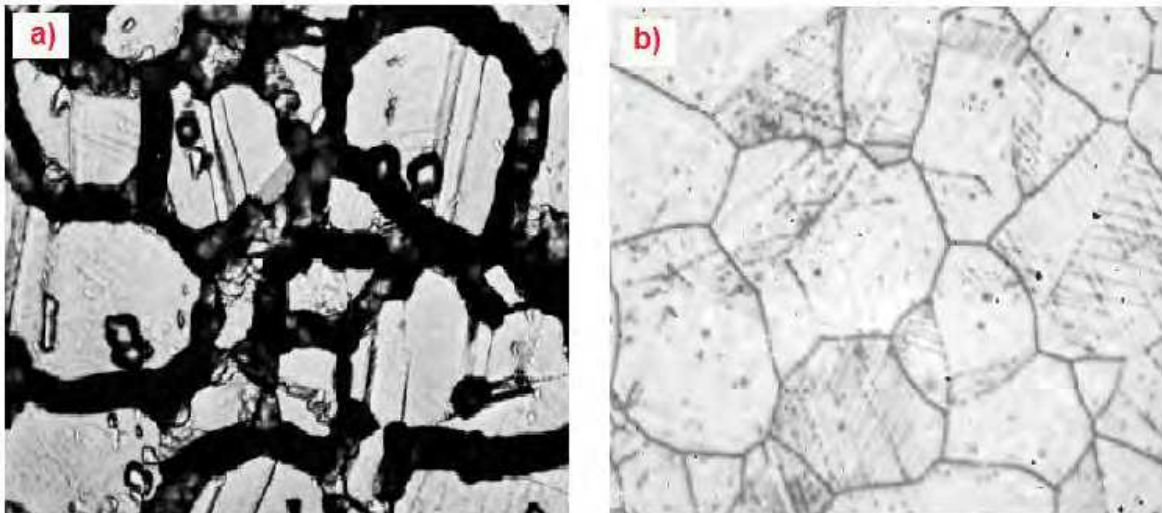


Fig. 6. Micrograph of sensitised austenitic stainless steel, a) sample of AISI 304 steel after high anodic polarisation in artificial seawater and b) sample after cyclic polarisation in $H_2SO_4$ + KSCN solution

Several electrochemical and non-electrochemical methods have been proposed and used to evaluate the degree of sensitisation of stainless steels. One of the most utilised is the electrochemical potentiokinetic reactivation test (EPR) based on Číhal's method (Číhal & Štefec, 2001).

Due to its quantitative nature and reproducibility, this method has been standardized by ASTM to estimate the sensitization grade of AISI type 304 and 304L stainless steels (ASTM, 1994).

Other research group proposed the double loop electrochemical potentiokinetic reactivation method (DLEPR) for determining the sensitization grade of stainless steels (Majidi et al., 1984). This author compared the results of the new method, the single loop and the acid test, and observed a wood agreement between measurement made with double loop and single loop EPR test giving a quantitative measure of sensitization based on the ratio of active peak currents on the forward and reverse scans Ir/Ia when the polarization is carried out in a 0.5 M $H_2SO_4$ + 0.01 M KSCN solution and a scan rate of 100 mV min-1.

Figure 7 presents the DLEPR curves of AISI 304 stainless steel for the case of samples taken from the heat affected zone (HAZ) after Gas metal arc welding (GMAW) and samples solution annealing at 1050 °C (red curve), (Curiel et al., 2011). The results obtained the DLEPR tests indicated clearly the effect of metallurgical condition of the stainless steel on its resistance to localised corrosion (intergranular). Samples of the HAZ presented a clear reactivation current density whereas the samples solution annealed showed just a negligible value of Ia. After the annealing treatment for 1 hr, not all Cr was dissolved completely, that is why there exists a small reactivation but several times lower than that for sensitised samples.

Electrochemical methods used to determine the sensitization intensity on stainless steels enjoyed wide expansion over the last 40 years, and the DL-EPR test has become one of the

most successful due to its quantitative nature and because can be considered as a non-destructive method.
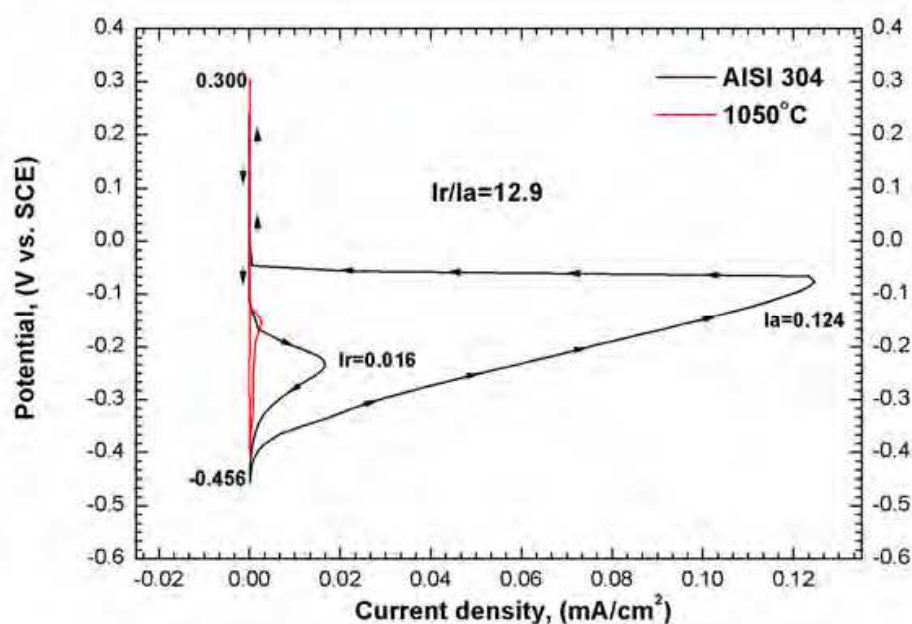


Fig. 7. DLEPR curves obtained from 304 SS samples at the HAZ after GMAW (black curve) and after solution annealing (red curve).

However as with any testing technique, attention must be paid in interpreting the results as measurements are sensitive to local changes in composition and microstructure of the alloy under study. In this sense, the use of alternative and reliable electrochemical technique has become o necessity in order to find the best way to determine the electrochemical behaviour of metallic materials or their corrosion resistance in diverse electrolytes.

During electrochemical reactions such as the corrosion of metals, electrochemical micro-cells form on the surface of the metal in contact with an electrolyte which induce potential and current fluctuations. These electrochemical fluctuations are known as Electrochemical Noise (EN) and definitively contain information about faradaic processes taking place on the electrified interface formed by a metal in contact with an electrolyte. In the second half of the 20th century there were numerous reports about the existence of these fluctuations (Iverson, 1968; Searson & Dawson, 1988). Several parameters are usually acquired from EN measurements which depend upon the method used for the data analysis (Gouveia-Caridade et al., 2004; Zaveri et al., 2007; Cottis & Turgoose, 1999). The results can be plotted as potential and current time series as the example shown in Figure 8.

Since the 90ties a preponderant importance has been given to the study of this phenomenon to explain the dynamics and mechanisms of the electrochemical processes taking place in the electrified interface (Gouveia-Caridade et al., 2004; Kearns et al., 1996; García-Ochoa et al., 1996; Hladky & Dawson, 1980; Loto & Cottis, 1987).

A number of procedures have been proposed and applied for the analysis of electrochemical noise data, from simple statistics analysis up to strategies that consider that pitting corrosion has a chaotic nature and apply non-linear methods to obtain parameters like the Lyapunov exponent (García et al., 2003).
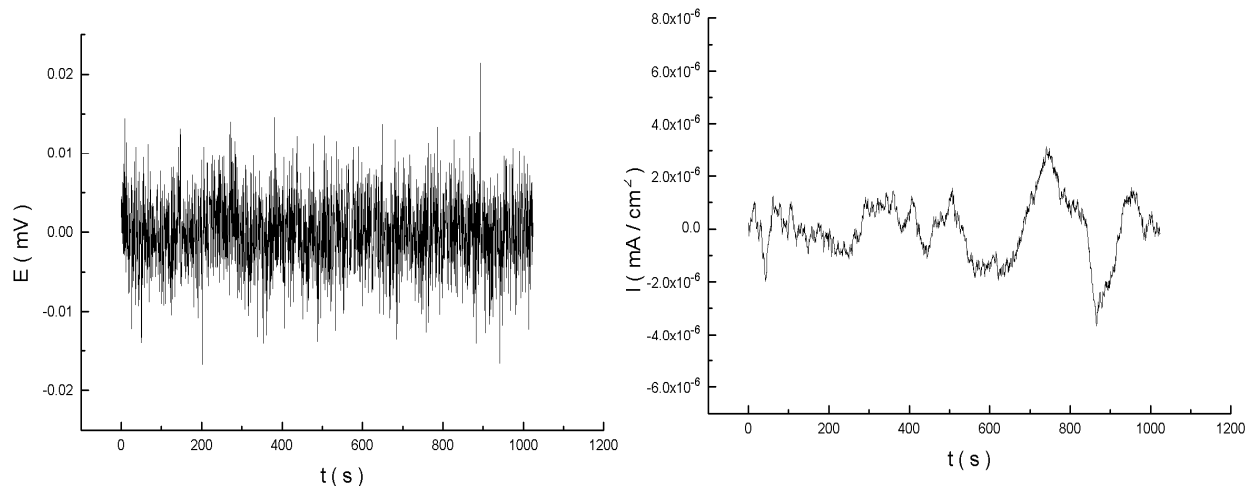
Fig. 8. Potential and current density time series obtained from electrochemical noise measurements.

Pitting corrosion studies conducted in the past using electrochemical noise measurements considered that high amplitude oscillations associated to breakdown - recovery of passive layers had a totally stochastic nature. Succeeding studies demonstrated that such approach was not correct because oscillations observed during the pitting of iron have a non-linear chaotic nature, this means processes of complex dynamics that are sensitive to initial conditions (García et al., 2003; González et al., 1997; Sazou & Pagitsas, 2003.

Visual recurrence analysis is another procedure to study the behaviour of nonlinear dynamical systems such as localized corrosion processes. This procedure has been used to differentiate between stochastic and chaotic variability. The principal instruments of the recurrence analysis are the Recurrence plots (RPs) which are especially useful for the graphical representation of multidimensional dynamic systems (Eckmann et al., 1987; Casdagli, 1998; Trulla, 1996). Recurrence plots (RPs) are a valuable tool for measure the geometry of the dynamics exploiting non-linear dependencies even in non-stationary time-series. These plots disclose distance relationships between points on a dynamical system providing a faithful representation of the time dependencies (correlations) contained in the data (Acuña et al., 2008). This is a graphical tool for the diagnosis of drift and hidden periodicities in the time evolution of dynamical systems, which are unnoticeable otherwise. Recurrence plots (RPs) are graphical tools elaborated by Eckmann et al. based on Phase Space Reconstruction (Eckmann et al., 1987). The method of RPs was introduced to visualize the time dependent behavior of the dynamics of systems, which can be pictured as a trajectory in the phase space as presented in Figure 9, (Zbilut & Webber, 1992; McGuire et al., 1997; Marwan et al., 2007).

This methodology was used also to study the dynamics of intergranular corrosion in austenitic stainless steel with different degree of sensitization (García-Ochoa et al., 2009).

The analysis of electrochemical noise in current using recurrence plots proved to be an excellent tool to evaluate the changes in the dynamics of the intergranular corrosion of AISI 304 austenitic stainless steel with different degree of sensitization. The RP´s showed that
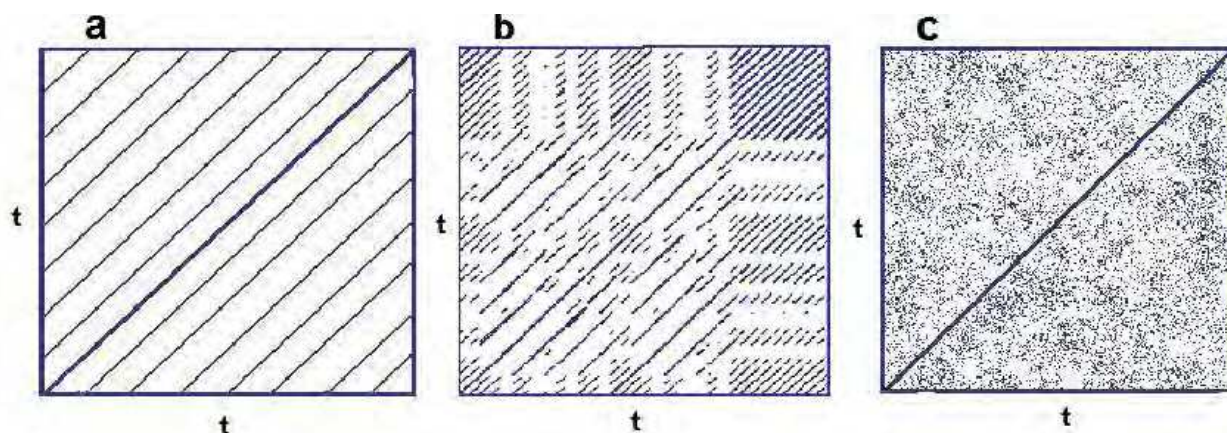
Fig. 9. Recurrence plots of (a) a periodic motion with one frequency, (b) the chaotic Rossler system and (c) of uniformly distributed noise (Marwan et al., 2007).

sensitisation causes a localised corrosion process with spatiotemporal well defined electrochemical cells interacting in the form of a dissolution process with periodic dynamics. The periodicity was determined by the increment of %D (percentage of determinism) and R% (the percentage of recurrence) as a function of the degree of sensitisation (DOS) (García-Ochoa et al., 2009).

Electrochemical noise measurements conducted during environmental assisted cracking of austenitic stainless steel detected changes in the electrochemical fluctuations which were associated to the cracking processes (Acuña, 2005; González et al., 1997). The methods applied to date for the analysis of electrochemical noise data to study the initial stages of corrosion fatigue damage (CFD) have been unable to separate the contribution due to localized corrosion from that due to crack nucleation and growth. Crack nucleation and growth involve generation of fresh active metal surfaces which interact with the electrolyte and induce changes in the amplitude of current fluctuations. This contribution to the noise signal must be different from that associated to the localised corrosion process which in principle should have dissimilar nature.

It was possible to separate the contribution of pitting corrosion for which electrochemical noise in current presented a percentage of determinism (%D = 80) higher than that associated to CF crack initiation which presented a stochastic behaviour with low %D (around 5%). This separation was possible by the use of the recurrence quantitative analysis parameter (RQA) selected: the percentage of determinism %D. Recursive Plots RPs applied to the analysis of electrochemical current noise measured during CF tests and their assessment by (RQA) represents a powerful non-linear analysis tool as it allowed us to establish clearly the dynamics of the early stages of CF cracking (Acuña et al., 2008).

### 3.2 Studies of localised corrosion using the Scanning Reference Electrode Technique (SRET)

The dissolution of metals during localised corrosion takes place at permanently separated sites from the bigger cathodic areas. This gives the possibility of direct measurements of the cathodic and anodic reactions through *in situ* non-intrusive studies. In order to study the kinetics of localised corrosion in its various forms it is necessary to use electrochemical

techniques capable to measure variations in electrochemical activity directly on the site undergoing localised attack at the metal surface.

Measurements of the physical separation of anodic and cathodic areas, the currents flowing between them as well as the mapping of potentials in electrolytic solutions have been successfully used for the study of the processes of localised corrosion of different systems (Isaacs & Vyas, 1981; Tuck, 1983; Bates et al., 1989; Sargeant et al., 1989; Trethewey et al., 1994; Trethewey et al., 1996; McMurra et al., 1996; McMurray & Worsley, 1996). A schematic drawing of a local corrosion cell is shown in figure 10.

With the aim of determining the velocity of metal dissolution directly in active pits during pitting corrosion, Rosenfeld and Danilov (Rosenfeld & Danilov, 1967), designed an apparatus to measure the field strength in the electrolyte directly above an active pit. They employed a twin probe method by using two reference electrodes, which makes it possible to measure the potential difference $\Delta E$ in any direction between two points in the electrolyte with the aid of two non-polarisable electrodes, for example calomel electrodes.
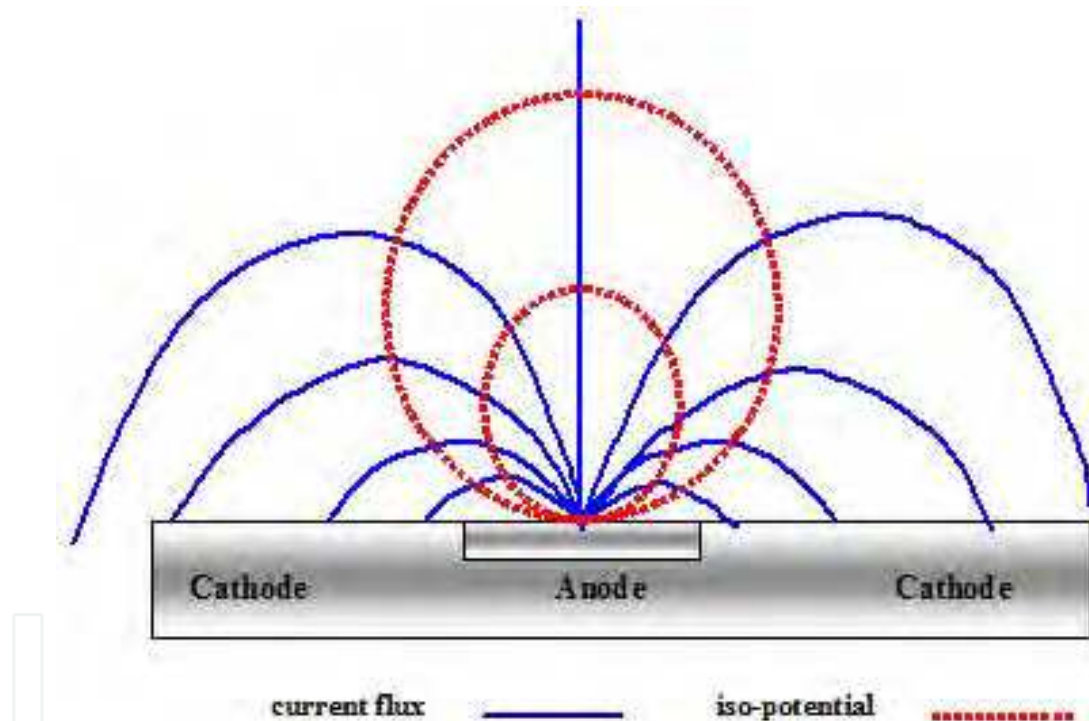


Fig. 10. Schematic of current and potential distribution in solution during localised corrosion

The equipment used for the measurements of the potential difference $\Delta E$ (ohmic potential gradients) is called the Scanning Reference Electrode (SRET). With the measurement of the electric field strength in the electrolyte over the pits it was possible to determine the current flowing from the anode points, based on the fact that, the vector of the normal component of the current density at a pre-determined point ($i'$) in a uniform field is equal to the product of the electric field strength E and the specific conductivity of the medium κ.

The resolution of the SRET depends upon the proximity of the scanning probes to the corroding sites and the magnitude of the corrosion currents from each site. As shall be shown later, the distance between the probe and specimen surface and the conductivity of

the solution governs the sensitivity of the technique. It has been reported the capability of the SRET to identify the position of localised activity in the metal surface however did not report any assessment of pit size or shape from the performed SRET measurements (Bates et al., 1989; Sargeant et al., 1989; Trethewey et al., 1994).

Tuck, (Tuck, 1983) evaluated the usefulness of reference microelectrodes in identifying local anodic and cathodic sites on aluminium alloys as they were scanned mechanically over a polished surface. The electrolyte in which the specimens were immersed for the study was shown to have a critical effect on the detectability of sites undergoing localised activity. He demonstrated that a solution of low conductivity is indispensable if the electrodes were microscopic in size. This is obviously a limitation in the application of microelectrodes because they cannot be used for real systems undergoing localised corrosion in electrolytes of high conductivity, e.g. seawater. Trethewey et al. (Trethewey et al., 1993) obtained pit life history at specific points in a 304 stainless steel specimen immersed in seawater. They showed that the measured current density adjacent to an active pit exceeded 300 times that obtained from a conventional pitting scan which was a maximum current density of 0.8 mA/cm$^2$. This author showed the advantages that in theory should give the use of a differential probe configuration over the conventional single ended system (Trethewey et al., 1994). The same authors indicated that with the use of SRET it is possible to study pit initiation and development, surface coating behaviour, inhibitor performance, battery performance, corrosion under hydrodynamic conditions as well as microbiological induced corrosion and stress corrosion cracking.

The SRET operation principle is based on the fact that during the localised corrosion of metals the electronic charge generated by the dissolution reaction flows from the localised anode to the cathodic sites through the metal. The high electronic conductivity of the metal induces a negligible ohmic potential difference in the metal, thus the surface of the corroding metal can be considered as a plane of constant potential. However within the aqueous electrolyte in contact with the corroding metal the ionic flow that develops to complete the corrosion cell produces ohmic potential gradients owing to the low electric conductivity of the electrolyte. As shown in figure 7, these potential gradients may be described as a series of iso-potential lines lying in perpendicular direction to the lines of ionic current flux. The activity can be assessed in terms of the current emanating from the sites undergoing local dissolution. By scanning a non-polarizable reference probe containing a fine capillary tip parallel and very close to the metal surface, the ohmic potential gradients generated in the electrolyte by localised anodic currents can be measured. It must be emphasised that the SRET does not directly measure the potential variations in the surface of the metal, but it responds to the ohmic potential gradients originated by ionic fluxes in the solution. SRET is a powerful equipment allowing real-time localised electrochemical activity to be managed and fully quantified.

From a study of pitting corrosion of austenitic stainless steel in artificial seawater SRET map scans were obtained which gave information about the electrochemical activity emanating from sites undergoing localised dissolution. A commercial SRET (Uniscan instruments model SR100) in which a cylindrical specimen (sealed tube or bar) is the working electrode, immersed in the electrolyte and rotated at precise speeds in the range 5–250 rpm was used.

Figure 11 presents a schematic of the SRET equipment used for the study.
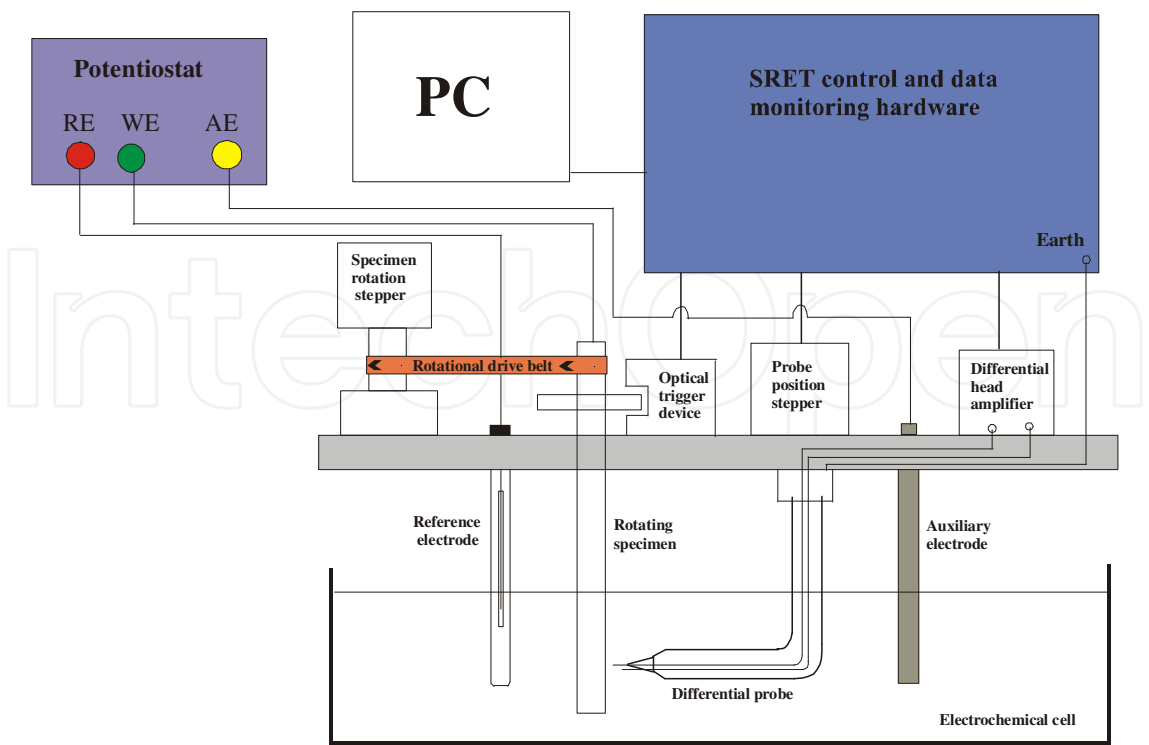
Fig. 11. Schematic representation of the SRET SR100.

A calibration procedure is mandatory and important aspect in order to assess the anodic current density associated with the ohmic potential gradient measured by the SRET. In this case a punctual source of current (a gold wire of 200 μm diameter) is immersed in the solution and polarised galvanostatically. The SRET measures a potential gradient which is then associated to the applied anodic current. A line scan and a map scan of the punctual source of current is presented in Figure 12.
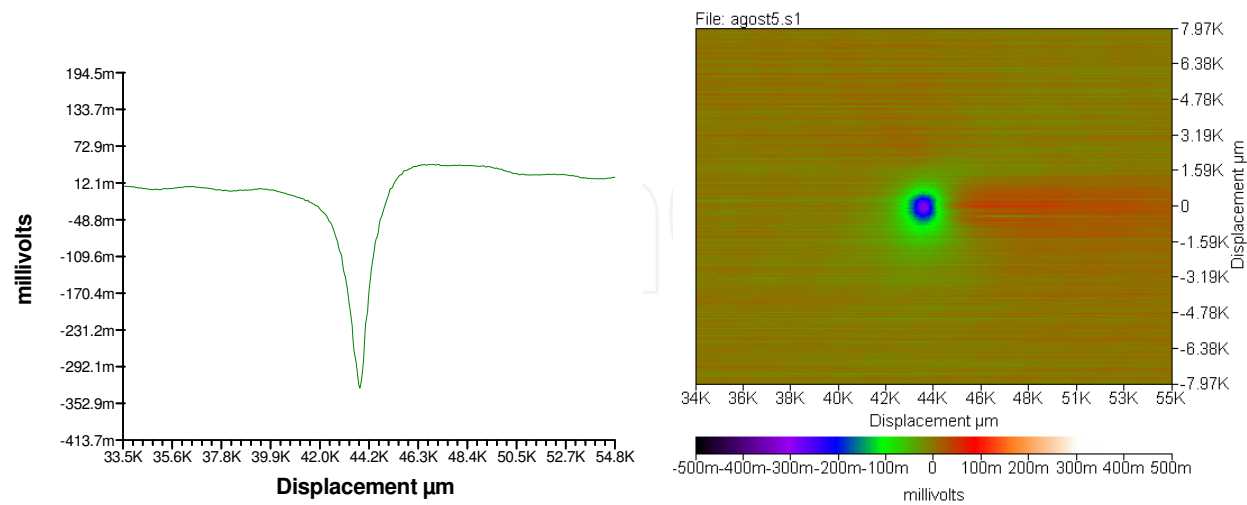


Fig. 12. Line and area map scans for a punctual current source in artificial seawater with an applied current density of i = 33.8 mA/cm$^2$, Maximum output signal = 0.327 mV.

Calibration experiments for the SRET showed that as the electrolyte conductivity increased, higher applied currents were needed in order to induce a signal detectable by the

equipment. In low conductivity electrolytes (0.014 mS/cm), the application of a current of 6.42 nA to a Punctual Current Source (PCS) was sufficient to generate a detectable signal.

However, in electrolytes with a conductivity of 55.8 mS/cm (3.5 wt% NaCl), the SRET detected a minimal output signal generated by applied currents higher than 3.73 mA as shown in Figure 13, (Dzib-Pérez et al., 2009).
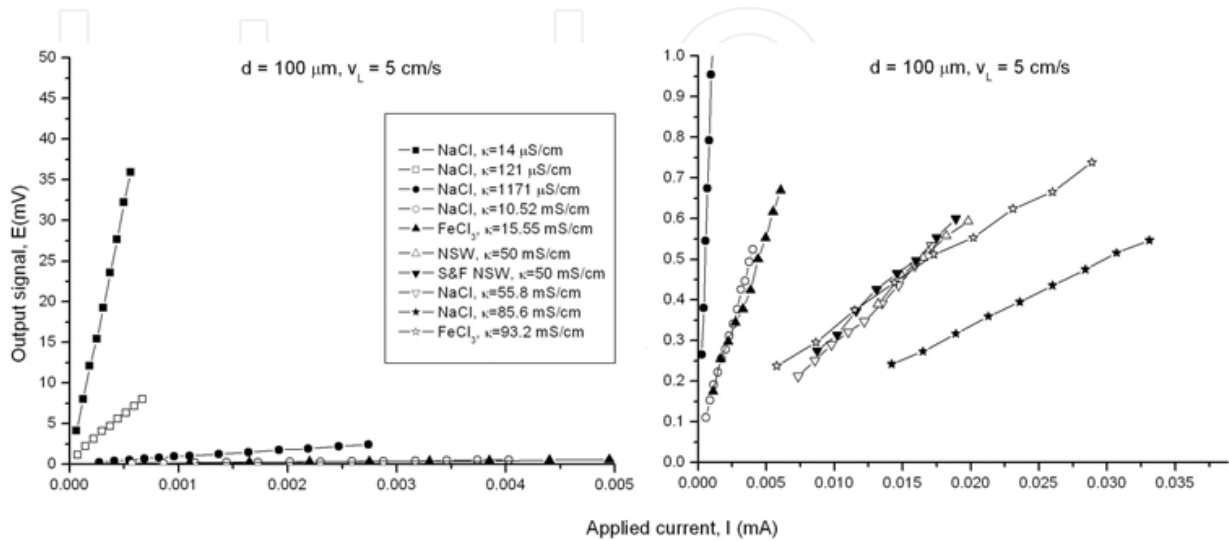


Fig. 13. Output signal vs applied current in electrolytes with different conductivity, 100 μm of separation surface-probe tip and a rotation rate of 5 cm/s. Magnification at the right to observe the response in high conductivity electrolytes.

The rotation rate of the working electrode has significant effect on the output signal for measurements in low conductivity electrolytes. The higher the rotation rate, the higher the slope of maximum signal detected vs applied current, which means better responsiveness (higher sensitivity of SRET) as shown in Figure 14.
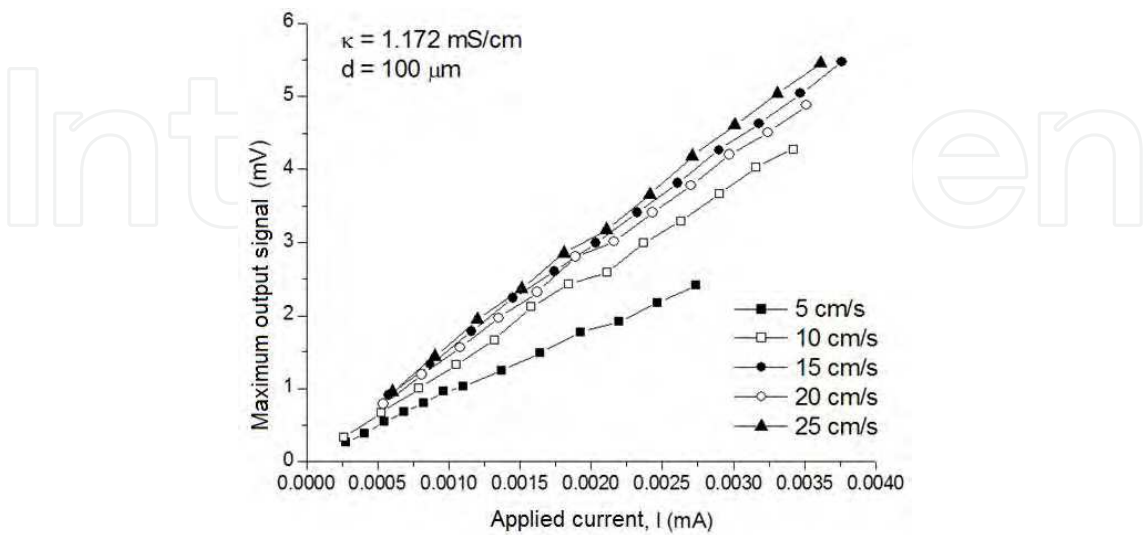


Fig. 14. Output signal vs applied current in NaCl solution (k = 1.172 mS/cm), with a separation probe tip to PCS of 100 μm and five different rotation rates.

Nevertheless, the resolution (WHM) of the SRET instrumentation decreases as the rotation rate increases. For the case of studies of localised corrosion in diluted electrolytes, this is a useful finding. It is of paramount importance an accurate understanding of the effects that operating parameters of the SRET equipment has on the measured output signal (Dzib-Pérez et al., 2009).

Studies of pitting corrosion of AISI 304 stainless steel in natural seawater were conducted performing SRET measurements on samples under cyclic anodic potentiodynamic polarisation from the open circuit potential to the repassivation potential as shown in Figure 15, (Dzib-Pérez, 2009; González-Sánchez, 2011). This study allowed quantitatively assessing the dissolution rate of stable pits and monitoring from initiation to repassivation (Dzib-Pérez, 2009).
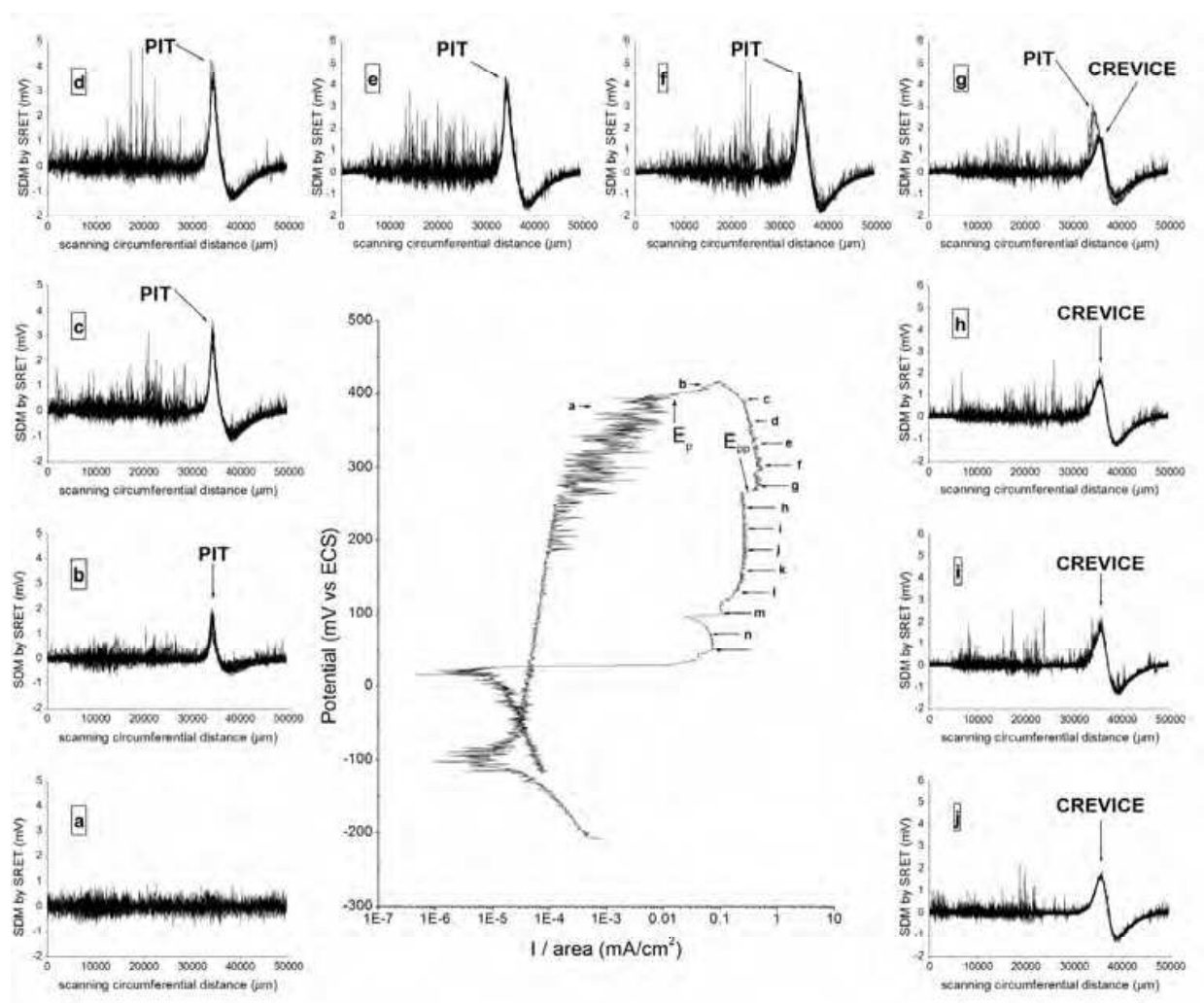


Fig. 15. SRET measurements conducted during potentiodynamic polarisation of AISI 304 stainless steel in natural seawater.

For a number of active pits generated on the AISI 304 stainless steel, measurements of the dissolved volume of metal per pit was determined by two methods. One was from material removal considering that pits had a spherical and elliptical geometry (Turnbull et al., 2006; González-Sánchez, 2002), and the second was done using SRET measurements of current density (Dzib-Pérez, 2009; González-Sánchez, 2002). By summing the SRET measured current density of the pit as a function of time and using Faraday´s law the quantity of dissolved metal was determined. The volume of dissolved metal per pit was calculated using the density of the AISI 304 stainless steel. The results showed acceptable agreement as can be seen in Figure 16.
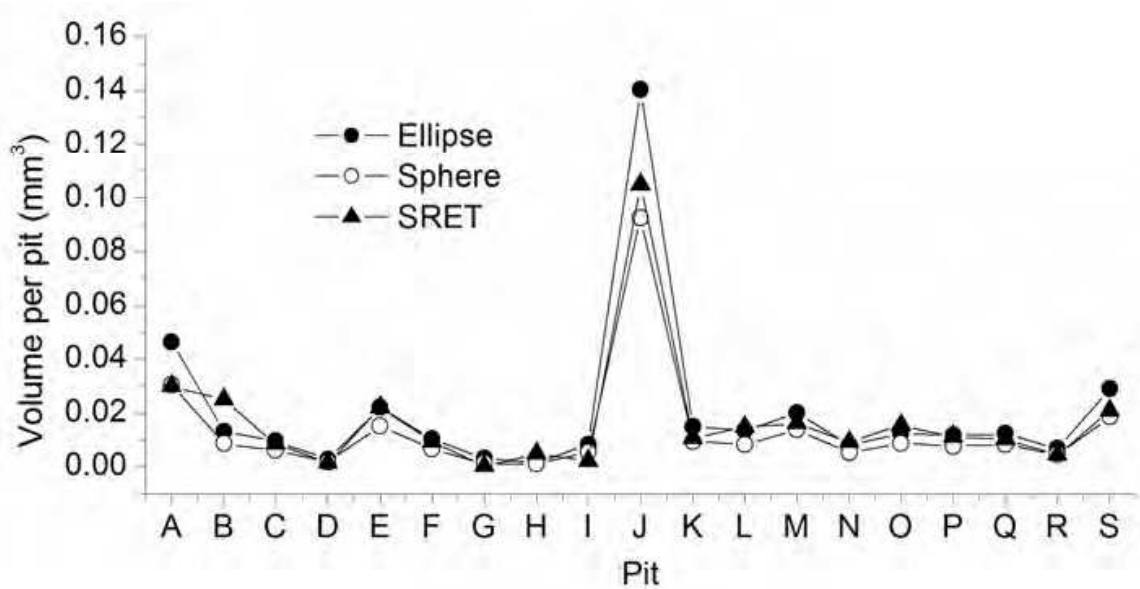


Fig. 16. Volume of dissolved metal per pit of AISI 304 stainless steel in natural seawater determined by material removal and SRET measurements.

Besides the capability of this technique to determine the position of the active pits, it is able to assess semi-quantitatively the dissolution rate in terms of localised current density. Calculations of the pit depth from the values of current density obtained from SRET agree well with the physical pit depth determined by material removal. SRET measurements showed that under potentiostatic control, active pit growth on 304 SS stainless steel in natural seawater takes place with an increase of localised current with time.

## 4. Conclusions

The degradation of engineering materials is a topic of paramount importance due to diverse forms in which the phenomenon takes place. From the apparently benign (non-aggressive) environment created by the atmosphere to really demanding media such as marine

conditions and sour gas and oil exploitation, conduction and processing, metals and alloys will face some kind of degradation. Also at high temperatures, chemical reactions take place producing metal degradation on dry conditions.

Electrochemical novel techniques as well as novel analysis methods are currently used in order to get an insight of the mechanisms of metals degradation in aqueous environments. Sensitive techniques like electrochemical noise are able to give information of changes in the dynamics of electrode reactions that take place during metallic corrosion. SRET measurements provide the possibility of quantitative, or at least semi-quantitative assessment of the localised dissolution rate in terms of current density.

On the other hand, the understanding of chemisorption of small gas molecules on transition metal surfaces is crucial to obtain a molecular level understanding of the mechanism of heterogeneous catalysis. From simulations at molecular level it was observed a metal bond weakening of 15% after CO adsorption. A detrimental effect on the metal bonds is observed after CO adsorption on the FeNi(111) surface and can be associated with the alloys embrittlement by decohesion mechanism.

## 5. Acknowledgment

## 6. References

Acuña, N. (2005). "Fatigue Corrosion Cracking of an Austenitic Stainless Steel using Electrochemical Noise Technique", *Anti. Corr. Meth. Mater.* Vol. 52, pp. 139-144.

Acuña, N., García-Ochoa, E., & González-Sánchez, J. (2008). Assessment of the dynamics of corrosion fatigue crack initiation applying recurrence plots to the analysis of electrochemical noise data *Int J Fatigue* Vol. 30, pp. 1211-1219

Akid, R., Dmytrakh, I. & Gonzalez-Sanchez, J. (2006). "Fatigue Damage Accumulation: The role of corrosion on the early stages of crack development", *Corros. Engng. Sci. & Techno*, Vol. 41, pp. 328-335.

ASTM Standards 1994, Standard G 108-94 In: Annual Book of, American Society for Testing and Materials, Philadelphia,PA, 1994, p. 444.

Bates, S., Gosden, S., & Sargeant, D. (1989). "Design and development of Scanning Reference Electrode Technique for investigation of pitting corrosion in FV 448 turbine disc steel", *Materials Science and Technology*, Vol. 5, pp. 356

Burstein, G., Liu, C., Souto, R., & Vines S. (2004). Origins of Pitting Corrosion, *Corros. Engng, Sci. Tech.* Vol. 39, pp. 25–32.

Casdagli, M. (1997). *Physica D* Vol. 108: 12

Číhal, V., & Štefec, R. (2001). *Electrochim Acta* Vol. 46, pp. 3867

Cook, D., Van Orden, A., Reyes, J., Oh, S., Balasubramanian, R., Carpio, J. & Townsend, H.(2000). Atmospheric corrosion in marine environments along the Gulf of Mexico, in: S.W. Dean, G. Hernández Duque-Delgadillo, J. Bushman (Eds.), Marine Corrosion in Tropical Environments, ASTM STP 1399, American Society for Testing and Materials, West Conshohocken, PA.

Corvo, F., Pérez, T., Martin, Y., Reyes, J., Dzib, L., González-Sánchez, J., & Castañeda, A. (2008). "Time of Wetness in tropical climate: Considerations on the estimation of TOW according to ISO 9223 standard", *Corros. Sci.*, Vol. 50, pp. 206-219.

Cottis, R., & Turgoose, S. (1999). Electrochemical impedance and noise. NACE, Houston, TX

Curiel, F., García, R., López, V., & González-Sánchez J. (2011). "Effect of magnetic field applied during gas metal arc welding on the resistance to localised corrosion of the heat affected zone in AISI 304 stainless steel, *Corros. Sci.*, Vol. 53, pp. 2393-2399.

Dzib-Pérez, L., González-Sánchez, J., Malo, J., & Rodríguez F. (2009). The effect of test conditions on the sensitivity and resolution of SRET signal response, *Anticorrosion Methods and Materials*, Vol. 56, No. issue 1, pp. 18-27

Dzib-Pérez, L., Ph.D. thesis, National Autonomous University of Mexico, Mexico, (2009).

Eckmann, J., Kamphorst, S., & Ruelle, D. (1987). Recurrence plot of dynamical system. *Europhys Lett* Vol. 4:973–7.

GajdoŠ, M., Eichler, A., & Hafner, J. (2004). CO adsorption of close-packed transition and Ninoble metal surfaces: trends from ab initio calculations. *J. Phys.: Condens. Matter.* Vol. 16, pp. 1141

García-Ochoa, E., González-Sánchez, J., Acuña, N., & Euan, J. (2009). Analysis of the dynamics of Intergranular corrosion process of sensitised 304 stainless steel using recurrence plots, *J. Applied Electrochem*, Vol. 39, pp. 637-645.

García-Ochoa, E., Ramírez, R., Torres, V., Rodríguez, F., & Genesca J. (2002). *Corrosion* Vol. 58, pp. 756.

García-Ochoa, E., González-Sánchez, J., Corvo, F., Usagawa, Z., Dzib-Pérez, L., & Castañeda, A. (2008). Application of electrochemical noise to evaluate outdoor atmospheric corrosion of copper after relatively short exposure periods, *J. Appl. Electrochem.*, Vol. 8 pp. 1363-1368.

García, E., Uruchurtu, J., & Genescá, J. (1996). *Afinidad* Vol. 53, pp. 215

García, E., Hernández, M., Rodríguez, F., Genescá, J., & Boerio, J. (2003). Oscilation and chaos in pitting corrosion of steel. *Corrosion* Vol. 59:50–8.

González, J., Salinas, V., García, E. & Díaz, A., (1997). Use Electrochemical Noise to detect the initation and propagation of stress corrosion cracks in 17-4 PH steel. *Corrosion* Vol. 53, pp. 693–699.

González-Sánchez, J. (2002). Corrosion fatigue initiation in stainless steels: The scanning reference electrode technique Ph.D. thesis, Sheffield Hallam University, U.K

González, J., Dzib, L., & Malo, J., Evaluation of pit dissolution rate on AISI 304 stainless steel with scanning reference electrode technique, (On preparation)

Grabke, H. (1998). Carburization: A High Temperature Corrosion Phenomenon, Elsevier, Amsterdam, The Netherlands.

Gouveia-Caridade, C., Pereira, I., & Brett, M., (2004). *Electrochim Acta* Vol. 49, pp. 785

Hladky, K., & Dawson, J. (1980). *Corros. Sci.* Vol. 21, pp. 317.

Hohenberg, P., & Kohn, W. (1964). *Phys. Rev.* Vol. 136, pp. B864–B871.

Isaacs H., The localised Breakdown and Repair of Passive Surfaces during Pitting, *Corros. Sci.* Vol. 29, pp. 313 – 323.

Isaacs, H., & Vyas, B. (1981). "Scanning Reference Electrode Techniques in Localised Corrosion", *Electrochemical Corrosion testing*, ASTM STP 727, p. 3, F. Mansfeld and U. Bertocci eds.

Itoh, J., Sasaki, T. & Ohtsuka, T. (2000). *Corros Sci* Vol. 42, pp. 1539

Iverson, W. (1968). *J. Electrochem. Soc.* Vol. 115, pp. 617

Jiang, D., Carter, E. (2004). Adsorption and dissociation of CO on Fe(110) from firstprinciples, *Surface Science* Vol. 570, pp. 167–177

Karmazyn, A., Fiorin, V., Jenkins, S., & King, D. (2003). First-principles theory and microcalorimetry of CO adsorption on the {211} surfaces of Pt and Ni, *Surface Science* Vol. 538, pp. 171–183

Kearns, J., Scully, J., Roberge, P., Reichert, D., & Dawson, J. (1996). Electrochemical Noise measurement for Corrosion Applications ASTM.

Lacombe, P., Baroux, B., & Beranger, G. (1993) Stainless steels. Les editions de physique, France

Loto, C., & Cottis, R. (1987). *Corrosion* Vol. 43, pp. 499.

Majidi, A., & Streicher, M. (1984). *Corrosion* Vol. 40, pp. 584

McGuire, G., Azar, N., & Shelhamer, M. (1997). Recurrence matrices and the preservation of dynamical properties. *Phys Lett A* Vol. 237:43–7. 29 December.

McMurray, H., Magill, S., & Jeffs, B. (1996). "Scanning Reference Electrode Technique as a tool for investigating localised corrosion phenomena in galvanised steels", *Iron and Steelmaking*, Vol. 23, No. Issue 2, pp. 183

McMurray, H., & Worsley, D. (1997). "Scanning Electrochemical Techniques for the Study of Localised Metallic Corrosion", in *Research in Chemical Kinetics*, Vol. 4, pp. 149, Compton & Hancock eds. Blackwell Science Ltd.

Marshall, P. (1984). "AUSTENITIC STAINLESS STEELS, Microstructure and Mechanical Properties", Elsevier Applied Science Publishers LTD, England.

Marwan, N., Carmen, M., Thiel, M., & Kurths, J. (2007). Recurrence plots for the analysis of complex systems, *Physics Reports* Vol. 438 pp. 237–329

Monkhorst, H. & Pack, J. (1976). *Phys. Rev. B.* Vol. 13, pp. 5188-5192.

Nakayama, S., Kaji, T., Shibata, M., Notoya, T., & Osakai, T. (2007). *J Electrochem Soc Vol.* 154, C1

Nakayama, S., Kimura, A., Shibata, M., Kiwabata, S., & Osakai T. (2001). *J Electrochem Soc* Vol. 148, B467

Newman, R. (2001). W.R. Whitney award lecture: understanding the corrosion of stainless steel, *Corrosion* Vol. 57, pp. 1030–1041.

Novak, P., Štefec, R., & Franz, F. (1975). *Corrosion* Vol. 31, pp. 344

Ordejon, P., Artacho, E., & Soler, J. (1996). *Phys. Rev. B.* Vol. 53, pp. R10441-R10444.

Perdew, J., Burke, K., & Ernzerhof, M. (1996). *Phys. Rev. Lett.* Vol. 77, pp. 3865-3868.

Peters, K., Walker, C., Steadman, P., Robach, O., Isern, H., & Ferrer, S. (2001). The adsorption of carbon monoxide on Ni(110) above atmospheric pressure investigated with surface X-ray diffraction. *Phys. Rev. Lett.* Vol. 86, pp. 5325

Rodriguez, N., Kim, M., Fortin, F., Mochida, I., & Baker, R. (1997). Carbon deposition on iron-nickel alloy particles, *Appl. Catal., A* Vol. 148, pp. 265–282.

Rosenfeld, I., & Danilov, I. (1967). "Electrochemical Aspects of Pitting Corrosion" *Corrosion Science*, Vol.7, pp.129.

Sánchez-Portal, D., Ordejon, P. & Canadell, E. (2004). Structure and Bonding, Vol. 113, pp. 103-170.

Sankey, O., & Niklewski, D. (1989). *Phys. Rev. B*. Vol. 40, pp. 3979-3995.

Sargeant, D., Hainse, J., & Bates, S. (1989). " Microcomputer controlled scanning reference electrode apparatus developed to study pitting corrosion of gas turbine disc materials ", *Materials Science and Technology*, Vol. 5, pp. 487

Sazou, D., & Pagitsas, M. (2003). Non-linear dynamics of the passivity breakdown of iron in acidic solutions. *Chaos Soliton Fract* Vol. 17:505–22.

Searson, P., & Dawson, J. (1988). *J. Electrochem. Soc.*, Vol. 135, No. issue 8, pp. 1908

Sudesh, T., Wijesinghe, L., & Blackwood D. (1989). Real time pit initiation studies on stainless steels: The effect of sulphide inclusions, *Corros. Sci.* Vol. 49 (2007) 1755 – 1764.

Soler, J., Artacho, E., Gale, J., Garcia, A., Junquera, J., Ordejon, P., & Sanchez, D. (2002). *J. Phys.: Condens. Matter* Vol. 14, pp. 2745-2779

Terada, M., Saiki, M., Costa, I., & Fernando, A. (2006). *J Nucl Mater* Vol. 358, pp. 40

Torres, V., Rodríguez, F., García-Ochoa, E. & Genesca, J. (2006). *Anticorros Meth Mater* Vol. 53, pp. 348

Trethewey, K., Sargeant, D., Marsh, D., & Haines, S. (1994). "New methods on quantitativeanalysis of localised corrosion using scanning electrochemical probes", in Modelling Aqueous Corrosion: From individual Pits to System management, p. 417, eds. K.R.

Trethewey, K., Sargeant, D., Marsh, D., & Tamimi, A. (1993). "Application of the Scanning Reference Electrode Technique to localised corrosion", *Corrosion Science*, Vol.35, No. issue 1-4, pp. 127.

Trethewey, K., Marsh, D., & Sargeant, D. (1996). "Quantitative Measurements of Localised

Corrosion Using SRET", *CORROSION-NACE 94*, Paper no. 317.Troullier, N., & Martins, J. (1991). *Phys. Rev. B*. Vol. 43, pp. 1993-2006.

Trulla, L., Giuliani, A., Zbilut, J., & Webber, C. (1996). *Phys Lett. A* Vol. 223: 255

Tuck, C. (1983). "The Use of Micro-electrodes in the Study of Localised Corrosion in Aluminium Alloys ", *Corrosion Science*, Vol. 23, No. issue 4, pp. 379

Turnbull, A., McCartney, L., & Zhou S. (2006). A model to predict the evolution of pitting corrosion and the pit-to-crack transition incorporating statistically distributed input parameters, *Corros. Sci.* Vol. 48, pp. 2084–2105.

Zaveri, N., Sunb, R., Zufelt, N., Zhoua, A., & Chenb, Y. (2007). *Electrochim Acta* Vol. 52, pp. 5795.

Zbilut, J., & Webber, C. (1992). Embedding and delays as derived from quantification of recurrence plot. *Phys Lett A* Vol. 171, pp. 199–203.

Zhou, S. & Turnbull, A. (1999). Influence of pitting on Fatigue life of Turbine Steel" *Fatigue Fract. Engng. Mater. Struct.* Vol. 22, pp. 1083 -1093.

Watanabe, M., Tomita, M. & Ichin, T. (2001). *J Electrochem Soc* Vol. 148, pp. B522
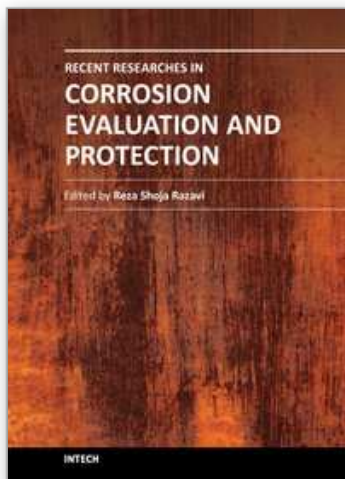
**Recent Researches in Corrosion Evaluation and Protection**

Edited by Prof. Reza Shoja Razavi

The purpose of this book is to present and discuss the recent methods in corrosion evaluation and protection. The book contains six chapters. The aim of Chapter 1 is to demonstrate that Electrochemical Impedance Spectroscopy can be a very useful tool to provide a complete evaluation of the corrosion protection properties of electro-coatings. Chapter 2 presents results of studies of materials degradation from experimental electrochemical tests and theoretical calculations. Chapter 3 deals with the presentation of the corrosion and corrosion prevention of the aluminum alloys by organic coatings and inhibitors. Chapter 4 addresses the new method of pigment preparation that can improve protection efficiency. The effectiveness of plasma deposited films on the improvement of carbon steel corrosion resistance is discussed in Chapter 5. Chapter 6 deals with the conjugation of carbon nanotubes with organic-inorganic hybrid to prepare hybrid coatings that combine high anti-corrosion efficiency with elevated mechanical resistance.

**How to reference**

In order to correctly reference this scholarly work, feel free to copy and paste the following:

Jorge González-Sánchez, Gabriel Canto, Luis Dzib-Pérez and Esteban García-Ochoa (2012). Application of Electrochemical Techniques and Mathematical Simulation in Corrosion and Degradation of Materials, Recent Researches in Corrosion Evaluation and Protection, Prof. Reza Shoja Razavi (Ed.), ISBN: 978-953-307-920-2, InTech, Available from: http://www.intechopen.com/books/recent-researches-in-corrosion-evaluation-and-protection/application-of-electrochemical-techniques-and-mathematical-simulation-in-corrosion-and-degradation-o

# INTECH

open science | open minds